Supporting Information for

Nano-makisu: highly anisotropic two-dimensional carbon allotropes made by weaving together nanotubes

Lei Zhao,[ab] Wei Liu,[cd] WenCai Yi,[e] Tao Hu,[bc] Dalar Khodagholian,[b] FengLong Gu,[f] Haiqing Lin,[d] Eva Zurek,[g] Yonghao Zheng,*[ah] Maosheng Miao*[bd]*

[a] *School of Optoelectronic Science and Engineering, University of Electronic Science and Technology of China (UESTC), Chengdu, 610054, P. R. China*

[b] *Department of Chemistry & Biochemistry, California State University Northridge, Northridge, CA, 91330, United States*

[c] *Department of Optical Engineering, Zhejiang A&F University, Hangzhou, 311300, P. R. China*

[d] *Beijing Computational Science Research Center, Beijing, 100193, P. R. China*

[e] *School of Physics and Physical Engineering, Qufu Normal University, Qufu, 273165, P. R. China*

[f] *Key Laboratory of Theoretical Chemistry of Environment, Ministry of Education, School of Chemistry and Environment, South China Normal University, Guangzhou, 510006, P. R. China*

[g] *Department of Chemistry, State University of New York at Buffalo, Buffalo, NY 14260-3000, United States*

[h] *Center for Applied Chemistry, University of Electronic Science and Technology of China (UESTC), Chengdu, 611731, P. R. China*

Table S1. Summary of energy differences per atom relative to graphene of Nano-makisu, Bubble-wrap carbon, and Egg-Tray Graphene.

Nano-makisu	ΔE/atom (eV)	Bubble-wrap carbon	ΔE/atom (eV)	Egg-Tray Graphene	ΔE/atom (eV)
M-30-h	0.80	B_1-T_1	0.81	T_1	0.24
M-30-to	0.89	B_1-T_2	0.76	T_2	0.25
M-40-h	0.55	B_1-H_1	0.72	H_1	0.33
M-40-to	0.60	B_1-H_2	0.69	H_2	0.25
M-50-h	0.39	B_1-H_3	0.65	H_3	0.22
M-50-to	0.43	B_2-T_1	0.75	H_4	0.25
M-60-h	0.29	B_2-T_2	0.70		
M-60-to	0.32	B_2-T_3	0.57		
		B_2-H_1	0.73		
		B_2-H_2	0.57		
		B_3-T_1	0.41		
		B_3-T_2	0.44		
		B_3-T_3	0.36		
		B_3-H_1	0.40		

Table S2. Summary of Fermi velocities of 2D Dirac carbon allotropes.

System		V_{Fx} (m/s)	V_{Fy} (m/s)
M-40-to	Point Ⅰ	8.11×10^5 3.22×10^5	1.80×10^4 1.68×10^4
	Point Ⅱ	7.80×10^5 4.01×10^5	4.56×10^3 1.08×10^5
	Point Ⅲ	8.43×10^5 7.11×10^5	2.14×10^4 2.18×10^4
M-40-h	Point Ⅲ’	8.44×10^5 5.73×10^5	7.89×10^5 4.74×10^5
M-60-to	Point Ⅰ	8.40×10^5 6.76×10^5	1.67×10^4 1.49×10^4
	Point Ⅱ	8.26×10^5 6.42×10^5	9.20×10^4 9.20×10^3
M-60-h	Point Ⅲ	8.03×10^5 3.09×10^5	5.32×10^4 4.34×10^4
α-graphyne[1]		6.77×10^5	6.77×10^5
β-graphyne[1]		3.87×10^5 4.35×10^5	6.77×10^5
6,6,12-graphyne[1]	Cone Ⅰ	5.56×10^5 6.29×10^5	6.04×10^5
	Cone Ⅱ	1.69×10^5	2.18×10^5
Phagraphene[2]		6.48×10^5	6.24×10^5 3.43×10^5
OPG-Z[3]		3.2×10^3	2.2×10^5
δ-graphyne[4]		6.96×10^5	6.96×10^5
S-graphene[5]	Cone Ⅰ	3.39×10^5	5.08×10^5
	Cone Ⅱ	3.63×10^5	4.35×10^5
D-graphene[5]		2.66×10^5	
E-graphene[5]		7.01×10^5	
S-graphynes[6]	4,12,4-graphyne	0.8×10^5	7.2×10^5
	4,12,2-graphyne	0.6×10^5	5.8×10^5
R-graphyne nanoribbons[7]		3.7×10^5	
$H_{4,4,4}$-graphyne[8]		$0.87\text{-}1.07\times 10^6$	
graphene		8.22×10^5	

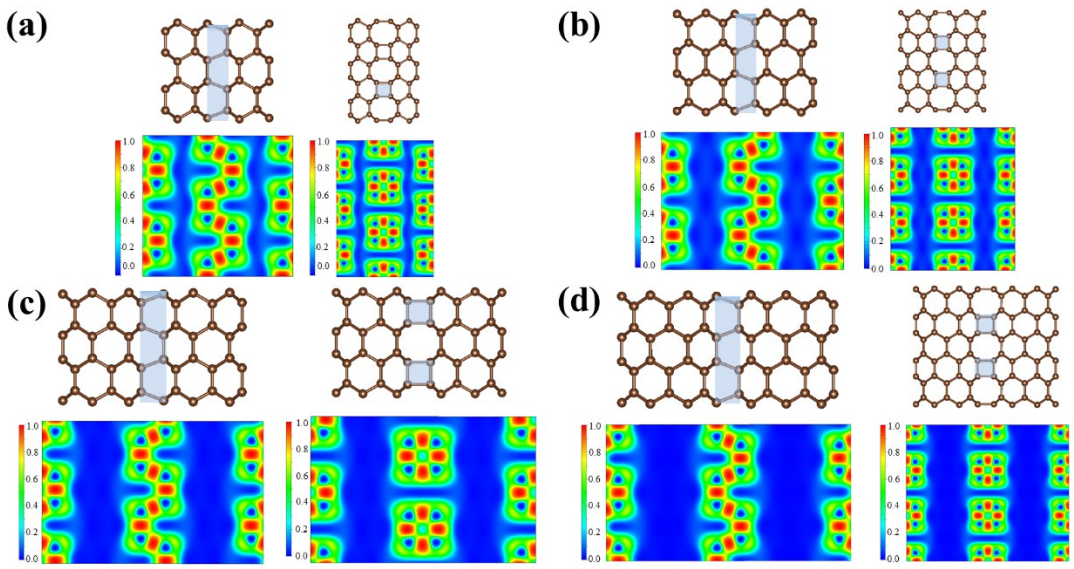

Fig. S1. The calculated ELF of nano-makisu (a) M-30-h/to; (b) M-40-h/to; (c) M-50-h/to; (d) M-60-h/to surface connecting two SWNTs. Blue to red indicates the gradually increased charge localization.

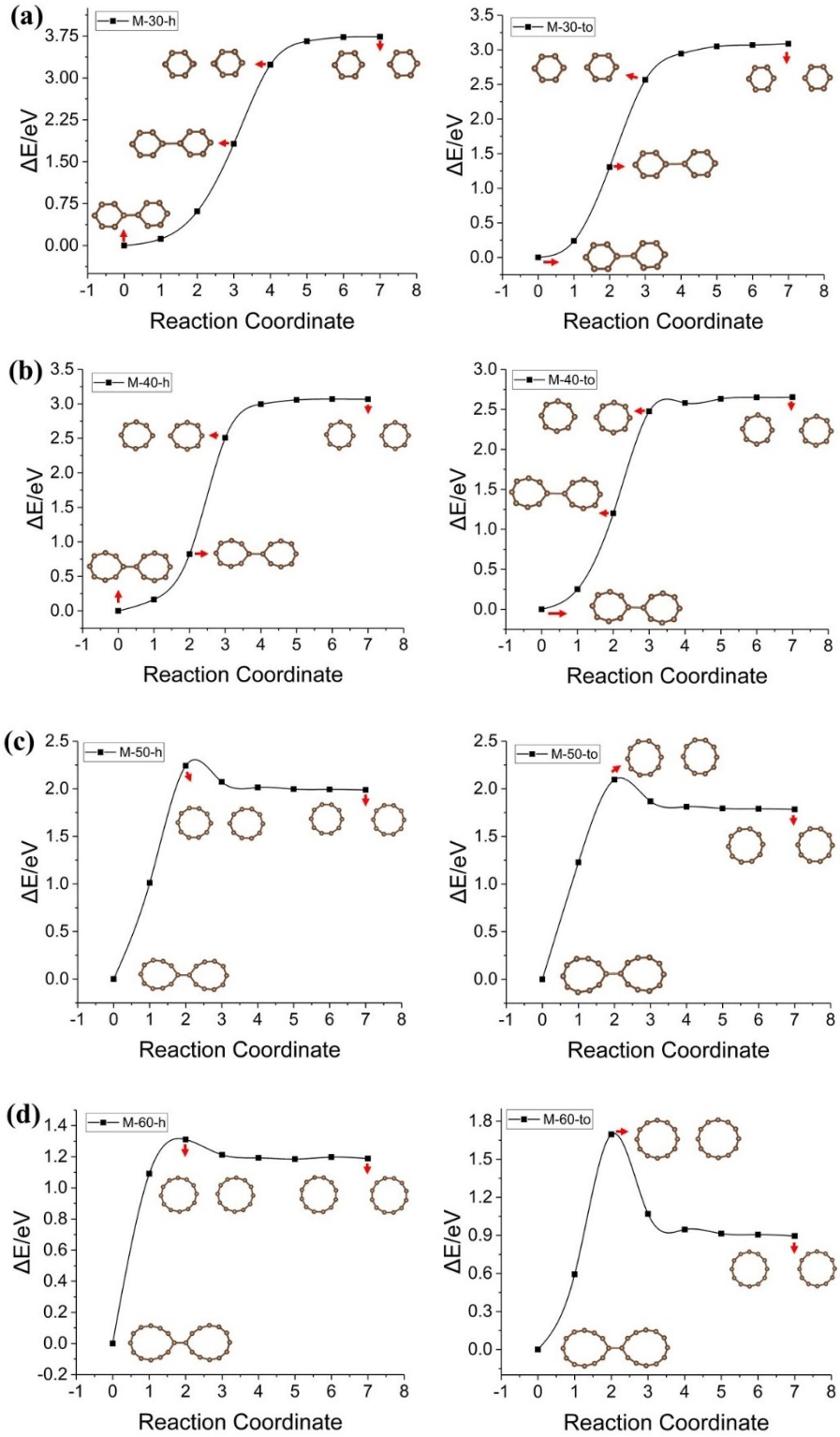

Fig. S2. Energy profiles of nano-makisu dissociation and corresponding geometric configurations. (a) M-30-h/to; (b) M-40-h/to; (c) M-50-h/to and (d) M-60-h/to.

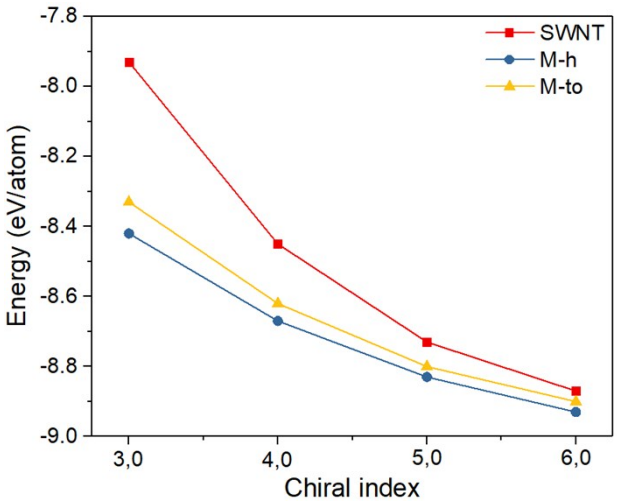

Fig. S3. Energy difference of nano-makisus with respect to parent SWNTs.

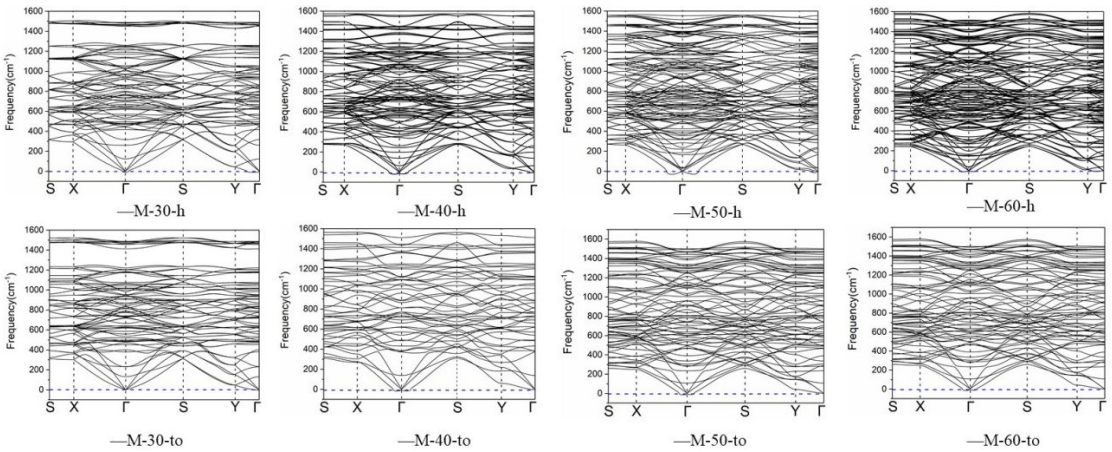

Fig. S4. The phonon spectra of nano-makisu.

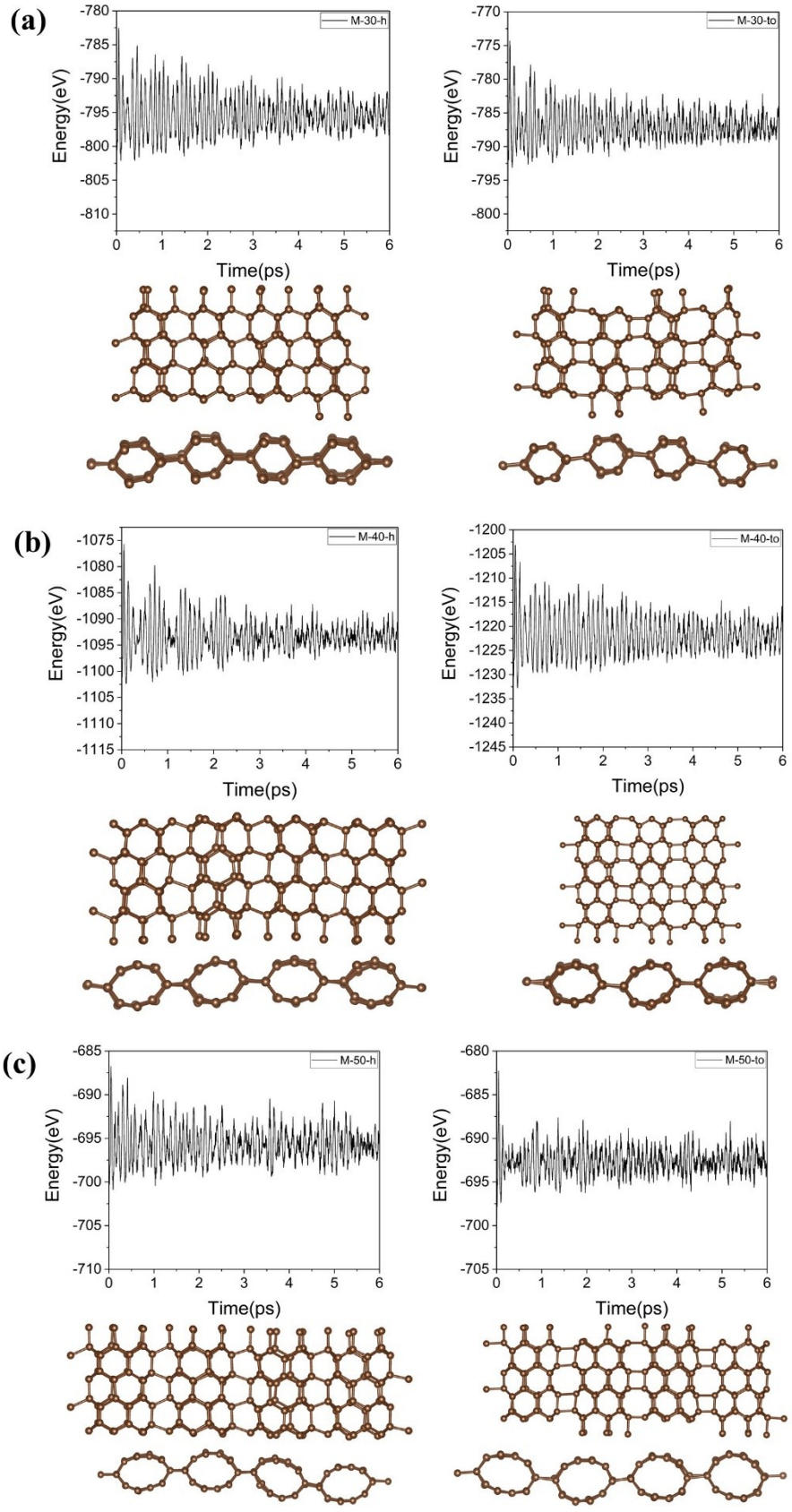
(a)
M-30-h
Energy(eV)
Time(ps)
M-30-to
Energy(eV)
Time(ps)
(b)
M-40-h
Energy(eV)
Time(ps)
M-40-to
Energy(eV)
Time(ps)
(c)
M-50-h
Energy(eV)
Time(ps)
M-50-to
Energy(eV)
Time(ps)

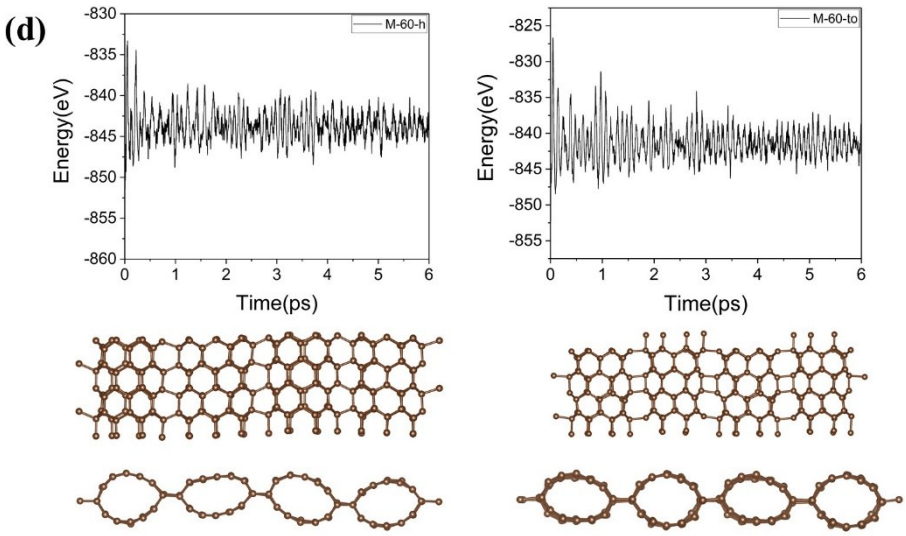

Fig. S5. Energy fluctuation and snapshots of the final configurations for each molecular dynamic simulation of nano-makisu at 1000 K after 6 ps. (a) M-30-h/to; (b) M-40-h/to; (c) M-50-h/to, and (d) M-60-h/to.

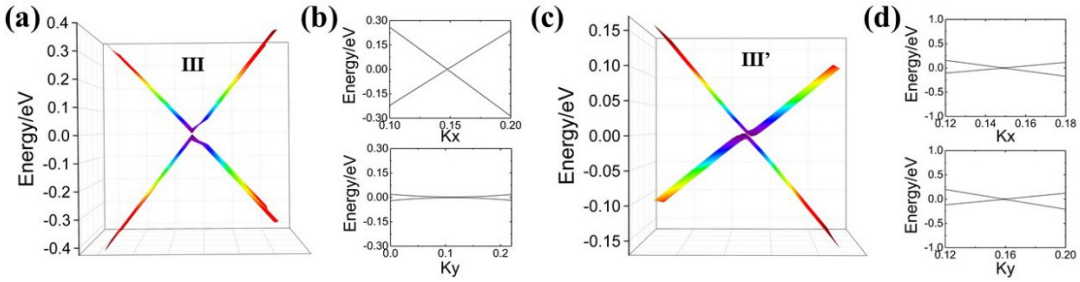

Fig. S6. (a) 3D Dirac cone formed by valence and conduction bands in the vicinity of the Dirac point Ⅲ in M-40-to; (b) Dispersions near the Dirac point Ⅲ parallel and perpendicular to the S-Y symmetry line; (c) 3D Dirac cone formed by valence and conduction bands in the vicinity of the Dirac point Ⅲ’ in M-40-h; (d) Dispersions near the Dirac point Ⅲ’ parallel and perpendicular to the S-Y symmetry line.

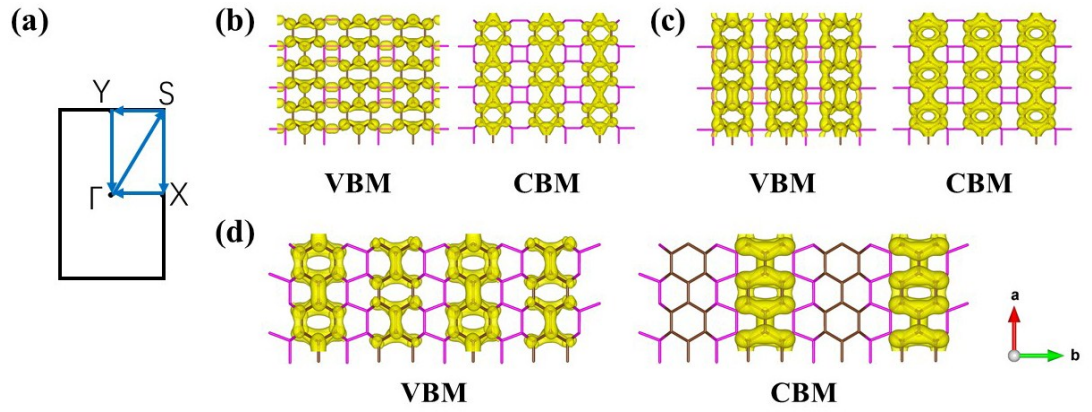

Fig. S7. (a) First BZ with letters representing special points and lines along which the band structure of nano-makisu is displayed; the band decomposed charge densities of the two Dirac bands in the proximity of the Fermi level at point I and II in M-40-to (b), point Ⅲ in M-40-to (c), and point Ⅲ' in M-40-h (d). Brown for sp^2-hybridized carbon atoms and pink for sp^3-hybridized carbon atoms. The isosurface value was set at 0.003 e/Å^3.

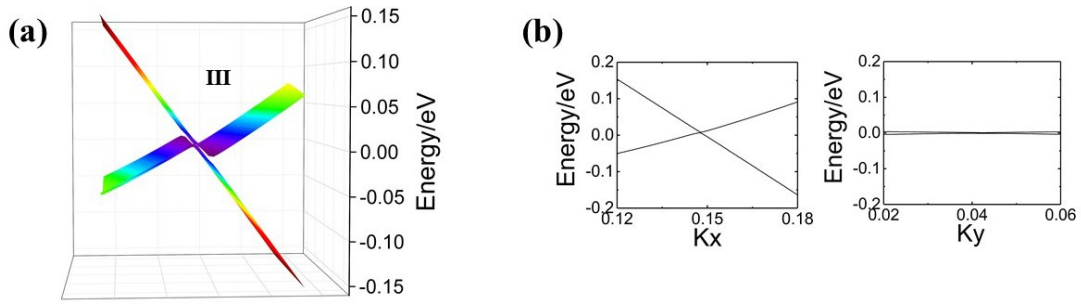

Fig. S8. (a) 3D Dirac cone formed by valence and conduction bands in the vicinity of the Dirac point Ⅲ in M-60-h; (b) Dispersions near the Dirac point Ⅲ in M-60-h parallel and perpendicular to the S-Y high symmetry line.

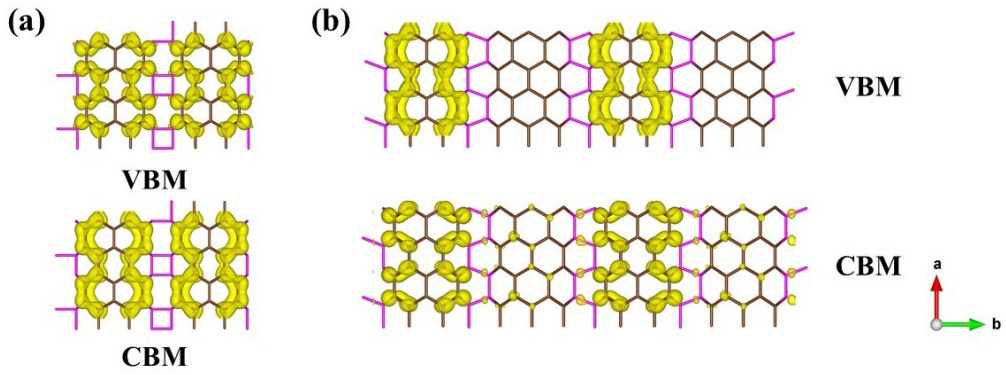

Fig. S9. The band decomposed charge densities of the two Dirac bands in the proximity of the Fermi level at point I and II in M-60-to (a) and point Ⅲ in M-60-h (b). Brown for sp^2-hybridized carbon atoms and pink for sp^3-hybridized carbon atoms. The isosurface value was set at 0.003 e/Å^3.

References

1. D. Malko, C. Neiss, F. Vines and A. Görling, *Phys. Rev. Lett.*, 2012, **108**, 086804.
2. Z. Wang, X.-F. Zhou, X. Zhang, Q. Zhu, H. Dong, M. Zhao and A. R. Oganov, *Nano Lett.*, 2015, **15**, 6182-6186.
3. C. Su, H. Jiang and J. Feng, *Phys Rev B*, 2013, **87**, 075453.
4. M. Zhao, W. Dong and A. Wang, *Sci rep*, 2013, **3**, 3532.
5. L.-C. Xu, R.-Z. Wang, M.-S. Miao, X.-L. Wei, Y.-P. Chen, H. Yan, W.-M. Lau, L.-M. Liu and Y.-M. Ma, *Nanoscale*, 2014, **6**, 1113-1118.
6. L. Zhang, Z. Wang, Z. M. Wang, S. Du, H.-J. Gao and F. Liu, *J Phys Chem Lett*, 2015, **6**, 2959-2962.
7. W.-J. Yin, Y.-E. Xie, L.-M. Liu, R.-Z. Wang, X.-L. Wei, L. Lau, J.-X. Zhong and Y.-P. Chen, *J Mater Chem A*, 2013, **1**, 5341-5346.
8. L. Li, X. Kong and F. M. Peeters, *Carbon*, 2019, **141**, 712-718.